Turkish J. Eng. Env. Sci.
32 (2008) , 1 – 5.

Numerical Computation of Fluid Flow in a Magnetohydrodynamic Micropump

H. M. DUWAIRI
University of Jordan, Mechanical Engineering Department, 11942 Amman-JORDAN
e-mail: duwairi@ju.edu.jo
Mustafa ABDULLAH
Al-Ahliyya Amman University, Faculty of Engineering, Amman-JORDAN

Received 24.01.2007

Abstract

A 2-dimensional model is developed to investigate fluid flow in a magneto-hydrodynamic (MHD) micropump. The transient, laminar, incompressible, and developing flow equations are numerically solved using the finite difference method and the SIMPLE algorithm. The micropump is driven using the Lorentz force, which is induced as a result of interaction between an applied electric field and a perpendicular magnetic field. The effect of Hartmann number on the transient velocity profile and the entrance region length is studied. It is found that controlling the electrical conductivity and magnetic flux density will allow controlling the entrance region length.

Key words: Magnetohydrodynamics (MHD), Micropump, Lorentz force.

Introduction

Many studies have been performed in micro-fluidic systems (Ngugen et al. 2002; Esashi, 1994). The magnetohydrodynamic (MHD) micropump is one of the important microfluidic systems that has no moving parts, generates continuous flow, and has potential applications in biomedical studies. The pumping source in MHD micropumps is the Lorentz force, which is produced as a result of an interaction between magnetic and electric fields.

Recent theoretical and experimental studies on DC and AC MHD devices were investigated. Lemoff et al. (1999) and Lemoff and Lee (2000) constructed a practical AC MHD pump in which the Lorentz force is used to propel an electrolytic solution along with a microchannel etched in silicon.

Eijkel et al. (2003) developed and fabricated an AC magnetohydrodynamic micropump for chromatographic application. Jang and Lee (2000) presented a DC micropump and obtained the performance of a MHD micropump in single phase using the simple model. The use of magnetohydrodynamic to circulate fluids in conduits fabricated with ceramic tapes was described by (Zhong et al., 2002).

To avoid gas bubbles, Homsy et al. (2005) described the operation of a DC MHD micropump at high current densities without introducing gas bubbles into the pumping channel. A new study of MHD flow is presented by Duwairi and Abdullah (2007). They studied theoretically the transient fully developed laminar flow and temperature distribution in MHD micropumps. The effect of different parameters on the transient velocity and temperature was presented.

In addition to MHD pumping, the study of mixing systems and microfluidic networks using MHD pumping has been performed. Lemoff and Lee (2003) used MHD forces to pump electrolytic solutions in microfluidic networks. Bau et al. (2001) and Yi et al. (2002) constructed and analyzed 2 types of magnetohydrodynamic stirrers experimentally and theoretically.

The above studies presented and analyzed differ-

ent models of the MHD micropump flow. In this paper, we studied numerically the transient developing flow in a magnetohydrodynamic (MHD) micropump.

Analysis

The MHD micropump consists of a channel of length L with a rectangular cross-section of width W and height h. A conductive liquid with a densityρ , a dynamic viscosityμ , and an electrical conductivity σ fills the channel.

The channel is subjected to a potential difference V imposed across the opposing electrodes that induces an electric current of density J. The channel is placed in a uniform magnetic field of flux density B in direction z.

The interaction between the magnetic and electric fields produces a body Lorentz force $\vec{J} \times \vec{B}$ that is perpendicular to both $\vec{J}$ and $\vec{B}$. The Lorentz force is used to pump the conducting liquids along the microchannel.

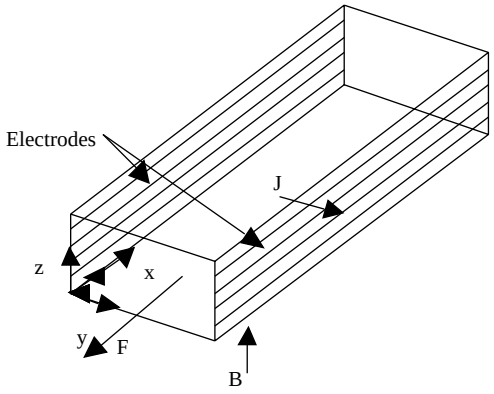

Figure 1. An inclined view of an MHD micropump.

Governing Equations

The governing equations of the MHD micropump that present the fluid motion are:

The Ohm's Law:

$$\vec{J} = \sigma \left(\vec{E} + \vec{u} \times \vec{B} \right) \tag{1}$$

The continuity equation:

$$\nabla . \vec{u} = 0 \tag{2}$$

The Navier-Stokes equation:

$$\rho \frac{\partial \vec{u}}{\partial t} + \rho \left(\vec{u} . \nabla \right) \vec{u} = -\nabla p + \mu \nabla^2 \vec{u} + \vec{J} \times \vec{B} \tag{3}$$

In our model, the width of the channel is assumed to be much larger than its height (w/h>>1), hence we studied the transient incompressible 2-dimensional developing flow. Figure 1 depicts schematically the channel's inclined view of the MHD micropump. A Cartesian coordinate system x,y with it's origin at the inlet is used. The coordinates x,y are aligned respectively along the channel's axis and width.

To develop the model, different assumptions are set as following:

1. Constant fluid properties
2. The current flow is assumed to be one dimensional
3. Laminar flow.

We used h, $u_0 = \sigma EBh^2/\mu$, $\sigma EBh$and h^2/ν as the length, velocity, pressure and time scales, respectively. The dimensionless form of continuity and Navier-Stokes equations for an incompressible, 2-dimensional developing flow become:

$$\frac{\partial u^*}{\partial x^*} + \frac{\partial v^*}{\partial y^*} = 0 \tag{4}$$

$$\begin{aligned} &\tfrac{\partial u^*}{\partial \tau} + \left(\tfrac{h}{L}\right) R_e \left(u^* \tfrac{\partial u^*}{\partial x^*} + v^* \tfrac{\partial u^*}{\partial y^*} \right) = \\ &-\frac{\partial p^*}{\partial x^*} + \frac{\partial^2 u^*}{\partial {x^*}^2} + \frac{\partial^2 u^*}{\partial {y^*}^2} + 1 + Ha^2 u^* \end{aligned} \tag{5}$$

$$\begin{aligned} &\frac{\partial v^*}{\partial \tau} + \left(\frac{h}{L}\right) R_e \left(u^* \frac{\partial v^*}{\partial x^*} + v^* \frac{\partial v^*}{\partial y^*} \right) = \\ &-\frac{\partial p^*}{\partial y^*} + \frac{\partial^2 v^*}{\partial {x^*}^2} + \frac{\partial^2 v^*}{\partial {y^*}^2} \end{aligned} \tag{6}$$

In the above equations, u^* and v^* are the dimensionless velocity components in x and y directions, τ is the dimensionless time, x^* and y^* are the dimensionless coordinates, $Ha = hB\sqrt{\frac{\sigma}{\mu}}$ is the Hartmann number, and $R_e = \frac{u_0 L}{\nu}$ is the Reynolds number. The boundary conditions can be specified as follows. The velocity is zero at all boundaries except the channel outlet:

$$\begin{aligned} &u^*(0, y^*) = v^*(0, y^*) = 0 \\ &u^*(x^*, 0) = v^*(x^*, 0) = 0 \\ &u^*(x^*, w/h) = v^*(x^*, w/h) = 0 \end{aligned}$$

The flow is fully developed at the channel outlet:

$$\frac{\partial u^*}{\partial x^*}\left(\frac{L}{h}, y^*\right) = \frac{\partial v^*}{\partial x^*}\left(\frac{L}{h}, y^*\right) = 0$$

Initially, at τ=0, $u^*(x^*, y^*) = v^*(x^*, y^*) = 0$

Method of solution

The nonlinear terms in the left hand side of the Navier-Stockes equations can be ignored because h/L<<1. The finite difference method and the simple algorithm (Patankar, 1980) are applied to solve the governing differential equations. A uniform grid in the x and y directions is used. The grid system has 1000 nodes in the x-direction and 200 nodes in the y-direction. The method with a large amount of time steps is employed until the steady state solution is achieved.

Results and Discussion

In this section, we studied the transient velocity profile, and discussed the effect of Hartmann number on the behavior of the transient velocity and the entrance length. To study the effect of this parameter, a numerical solution for the velocity profile is computed for different values of Hartmann number.

Figures 2 and 3 illustrate the effect of Hartmann number on the velocity profile and the entrance region length. It is seen that the mid-width velocity components U and V decrease as the Hartmann number increases, which means that a slightly conductive fluid is enough to propel the fluid. It is also seen that the axial velocity U increases and the velocity component V decreases until they reach the fully developed region, which is influenced by the Hartmann number. This means that controlling the electrical conductivity and magnetic flux density will allow controlling the entrance region length.

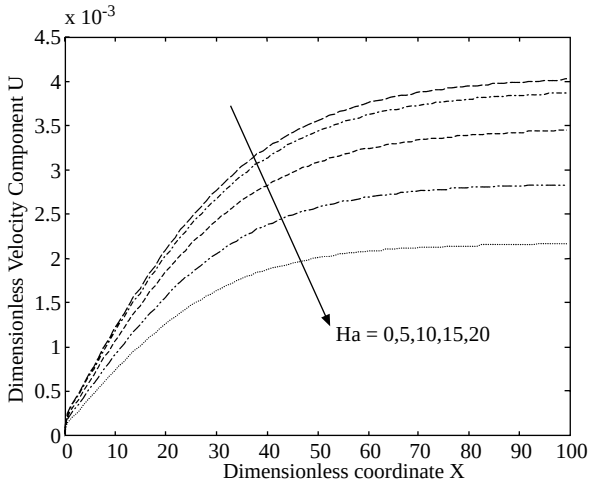

Figure 2. Variation of the dimensionless mid-width axial velocity U with the dimensionless X coordinate at different Hartmann numbers.

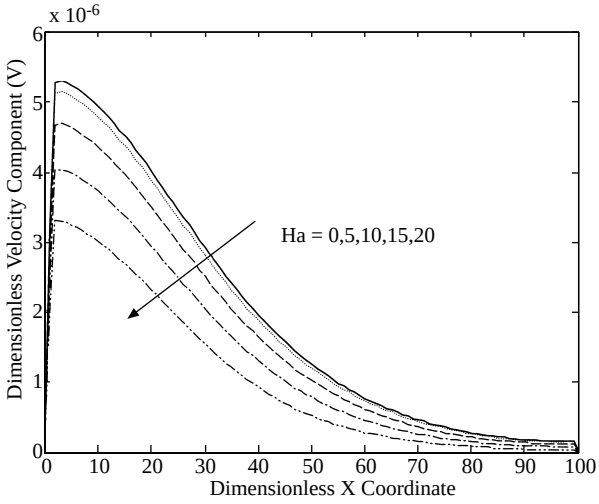

Figure 3. Variation of the dimensionless mid-width velocity component V with the dimensionless X coordinate at different Hartmann numbers.

Figure 4 depict the dimensionless pressure P which decreases as the Hartmann number increases. It is noticed that the pressure increases at the channel inlet and then decreases until reaching a constant pressure gradient at the channel fully developed region.

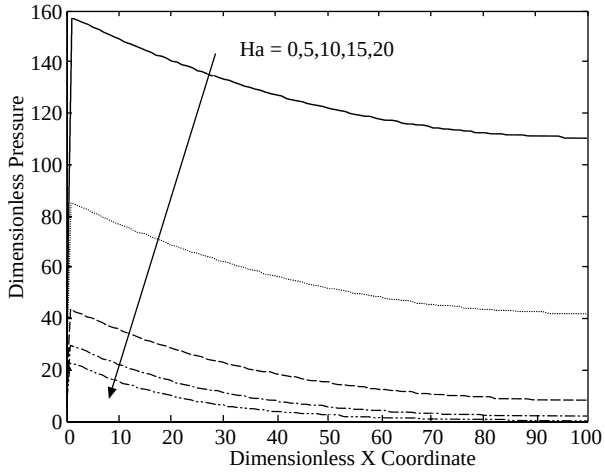

Figure 4. Variation of the dimensionless pressure P with the dimensionless X coordinate at different Hartmann numbers.

The variation of velocity components U and V with the dimensionless Y coordinate is shown in Figures 5 and 6 at different Hartmann numbers. It is seen that at low Hartmann number, the axial velocity (U) profile is parabolic, and as the Ha increases,

the profiles flattens. From Figure 6 it is seen that maximum velocity (V) reached at the end of the first and third quarter of the channel width.

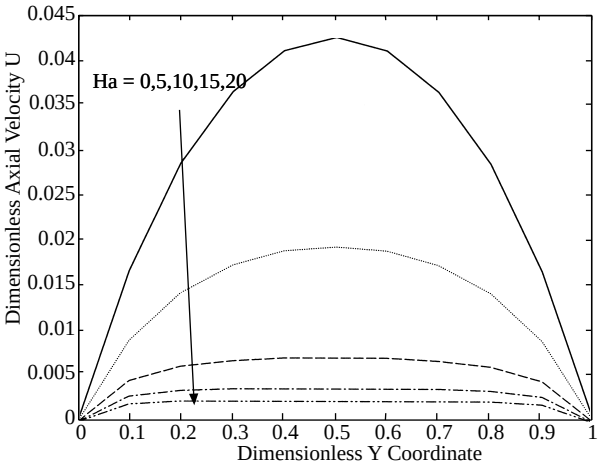

Figure 5. Variation of the dimensionless mid-length axial velocity U with the dimensionless Y coordinate at different Hartmann numbers.

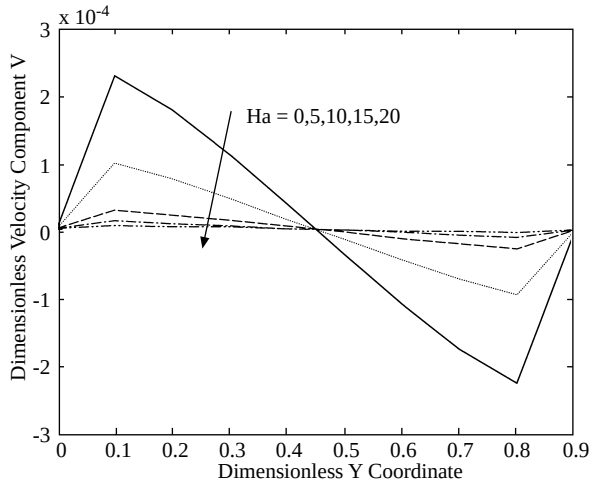

Figure 6. Variation of the dimensionless mid-length velocity component V with the dimensionless Y coordinate at different Hartmann numbers.

The effect of Hartmann number on the transient behavior of the mid-width dimensionless centerline velocity components U and V is shown in Figures 7 and 8. It is seen that the effect of increasing Ha decreases the time required to reach steady state.

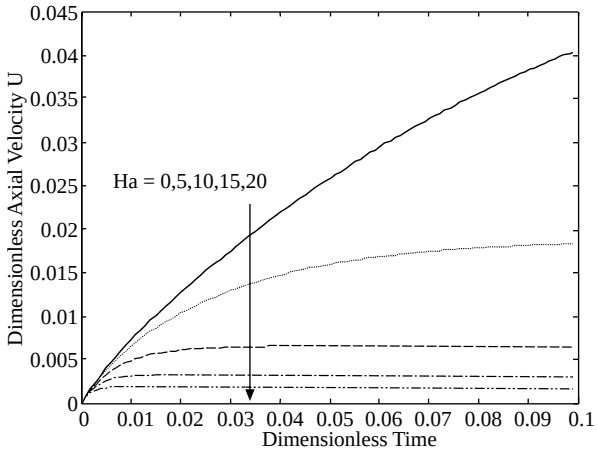

Figure 7. Transient behavior of the mid-length centerline axial velocity U at different Hartmann numbers.

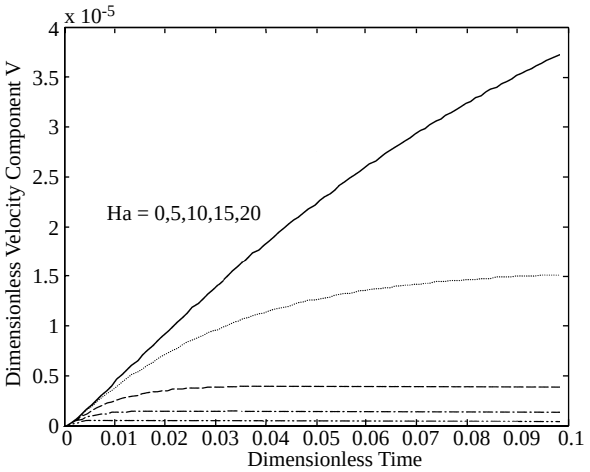

Figure 8. Transient behavior of the mid-length centerline velocity component V at different Hartmann numbers.

Conclusion

A numerical method to predict the velocity distribution in a magnetohydrodynamic (MHD) micropump has been proposed. In this study, the effect of Hartmann number on the transient velocity profiles is investigated. It is noticed that controlling the velocity profile and the entrance length can be achieved by controlling the potential difference, the magnetic flux, and by a good choice of the electrical conductivity.

Nomenclature

B	magnetic flux density (Tesla)
E	electric field intensity (volt/m)
h	height of micro-channel (m)
Ha	Hartman number, $Ha = hB\sqrt{\sigma/\mu}$
J	electric current density (Amper/m^2)
L	length of micro-channel (m)
P	pressure (N/m^2)
p^*	dimensionless pressure
t	time (s)
u,v	velocity components in the x and y directions
u^*, v^*	dimensionless velocity components in x and y directions
V	potential difference (volts)
w	width of microchannel (m)
x, y, z	Cartesian coordinates
x^*, y^*	dimensionless coordinates

Greek Symbols

μ	dynamic viscosity ($N \cdot s/m^2$)
ρ	density (Kg/m^3)
υ	kinematic viscosity (m^2/s)
σ	liquid's conductivity ($Siemens/m$)
τ	dimensionless time

References

Bau, H., Zhong, J. and Yi, M., "A Minute Magneto Hydro Dynamic (MHD) Mixer", Sensors and Actuators. 79, 207–215, 2001.

Duwairi, H. M. and Abdullah, M., "Thermal and Flow Analysis of a Magnetohydrodynamic Micropump", Microsystem Technologies, 13:1, 33-39, 2007.

Eijkel, J., Dalton, C., Hayden, C., Burt, J. and Manz, A, "A Circular Ac Magnetohydrodynamic Micropump For Chromatographic Applications", Sensors and Actuators, 92, 215-221, 2003.

Homsy, A., Koster, S., Eijkel, J., Berg, A., Lucklum, F., Verpoorte, E. and Rooij, F., "A High Current Density DC Magnetohydrodynamic (MHD) Micropump", Lab Chip, 5, 466-471, 2005.

Jang, J. and Lee, S., "Theoretical and Experimental Study Of MHD (Magnetohydrodynamic) Micropump", Sensors and Actuators, 80, 84–89, 2000.

Lemoff, A., Lee, A., Miles, R. and McConaghy, C., "An AC Magnetohydrodynamic Micropump: Towards a True Integrated Microfluidic System",Int. Conf. on Solid-State Sensors and Actuators (Transducers '99), 1126–1129, 1999.

Lemoff, A. and Lee, A.,"An AC Magnetohydrodynamic Micropump", Sensors and Actuators. 63, 178–185, 2000.

Lemoff, A. and Lee, A., "An Ac Magnetohydrodynamic Microfluidic Switch for Micro Total Analysis Systems", Biomedical Microdevices, 5:1, 55-60, 2003.

Nguyen, N., Huang, X. and Chuan, T.,"MEMS-Micropumps: A Review", Transactions of the ASME, 124, 384-392, 2002.

Patankar, S., "Numerical Heat Transfer and Fluid Flow", Hemisphere, Washington DC, 1980.

Shoji, S. and Esashi, M., "Microflow Devices And Systems", J. Micromech.Microeng. 4, 157-171, 1994.

Yi, M., Qian, S. and Bau, H.(2002), "A Magnetohydrodynamic Chaotic Stirrer", J. Fluid Mech.468, 153-177, 2002.

Zhong, J. Yi, M. and Bau, H., "Magneto Hydrodynamic (MHD) Pump Fabricated With Ceramic Tapes", Sensors and Actuators, 96, 59–66, 2002.